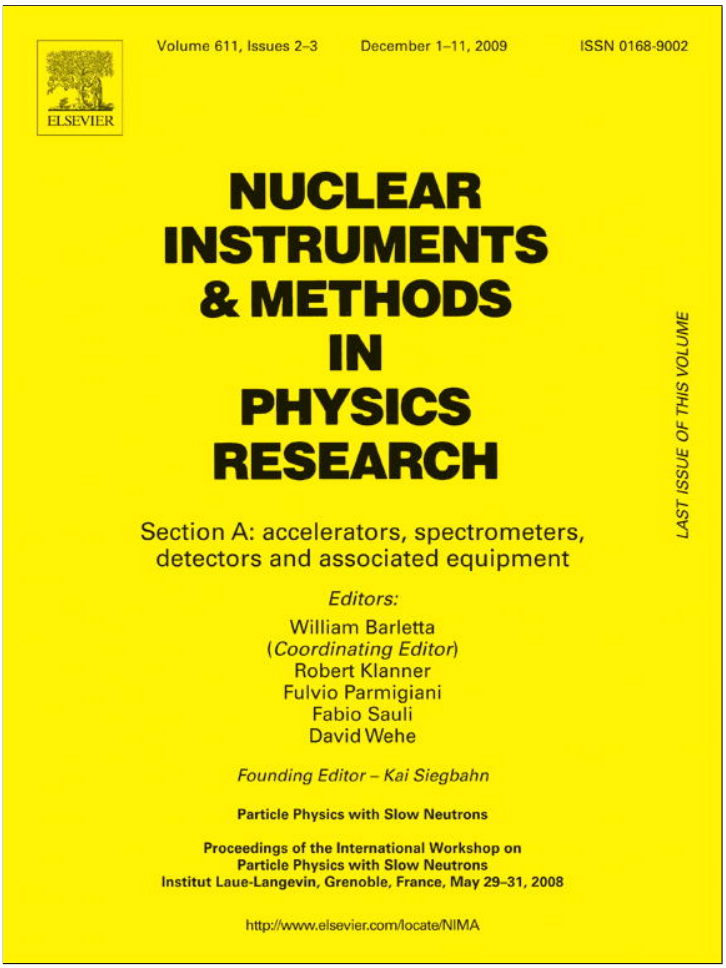

Nuclear Instruments and Methods in Physics Research A 611 (2009) 302–305

Contents lists available at ScienceDirect

Nuclear Instruments and Methods in Physics Research A

journal homepage: www.elsevier.com/locate/nima

Coherent scattering of slow neutrons at nanoparticles in particle physics experiments

E.V. Lychagin [a], A.Yu. Muzychka [a], V.V. Nesvizhevsky [b,*], G.V. Nekhaev [a], G. Pignol [c], K.V. Protasov [c], A.V. Strelkov [a]

[a] JINR, 6 Joliot-Curie, Dubna, Moscow reg., 141980, Russia
[b] ILL, 6 rue Jules Horowitz, F-38042 Grenoble, France
[c] LPSC (UJF, CNRS/IN2P3, INPG), 53, rue des Martyrs, F-38026 Grenoble, France

ARTICLE INFO

Available online 7 August 2009

Keywords:
Slow neutrons
Nanoparticles
Neutron scattering
Fundamental particle physics

ABSTRACT

Usually Ultra Cold Neutrons (UCN) and Very Cold Neutrons (VCN) are not efficiently scattered by individual atoms in matter due to their large wavelength. On the contrary, such neutrons are coherently scattered by nanoparticles, providing a powerful tool, in particular for VCN reflectors, for VCN storage in closed traps, probably for 'quasi-specular' reflectors for cold neutrons, and for cooling VCN to the UCN energy range. On the other hand, quasi-elastic scattering of UCN at nanoparticles and large molecules (as those of Fomblin oil) in all presently used UCN trap wall materials causes false effects in the neutron lifetime measurements because of poorly controlled spectrum evolution.

1. Introduction

Slow neutrons, in particular Ultra Cold Neutrons (UCN, $E<10^{-7}$ eV) and Cold Neutrons (CN, 10^{-4} eV$<E<10^{-2}$ eV), provide an excellent tool for various high-sensitive experiments such as searches for non-zero neutron electric dipole moment [1,2] or electric charge [3,4], precision studies of the neutron β-decay [5–7], experiments with the gravitationally bound quantum states of neutrons [8,9], and studies of fundamental symmetries [10,11]. The intermediate range of Very Cold Neutrons (VCN, 10^{-7} eV $<E<10^{-4}$ eV) has not been widely used in this field. However, any progress in the mentioned experiments followed always from preceding methodical developments. In Section 2 we present a new approach that allows us to apply the experimental methods typical for UCN to the VCN energy range. It is based on efficient coherent scattering of VCN on nanoparticles and nanostructures. In particular, we studied VCN reflection from powders of diamond nanoparticles [12–25] and storage of VCN in closed traps with walls built of such powders. The strongly bound nanoparticles of diamond in powder provide essentially elastic reflection. VCN storage in traps might be used for constraining the neutron electric dipole moment [44] or for measuring the neutron–neutron scattering length [40]. VCN reflectors would increase considerably UCN/VCN/CN fluxes for traditional particle experiments, thus improving their sensitivity. Shaping of VCN beams using nanostructured reflectors might be used, for instance, in neutron scattering experiments constraining short-range interactions [45].

In contrast to that case, weakly bound nanoparticles on surfaces considered in Section 3 reflect neutrons quasi-elastically. These studies were initially motivated by efforts to maximize the storage time of UCN in traps. Since the discovery of UCN [26], neutron losses from traps have always exceeded the theoretically expected values [27–31]. In 1997 an additional mechanism for UCN losses was observed: the UCN energy increased by $\sim 10^{-7}$ eV with the probability of 10^{-8}–10^{-5} per collision [12,13]. This process has been studied on solid and liquid surfaces [12–15,18,25,32–36]. Results presented in Ref. [22] agree with a hypothesis [17] that small heating of UCN on solid surfaces results from the coherent scattering of UCN on weakly bound nanoparticles on a surface in a state of thermal motion. Here we present new results indicating that nanoparticles are formed on solid surfaces due to surface heating. The temperature of their formation was found to be equal to the temperature of strong increase in the probability of small heating of UCN.

In all these cases the reason for a significant interplay between particle physics with slow neutrons and the physics of nanoparticle consists in an approximate equality of some characteristic parameters [17]: the neutron wavelength is close to the nanoparticle size; simultaneously the neutron velocity is close to the nanoparticle thermal motion velocity.

2. Efficient reflection of VCN at nanoparticle powders

Powders of nanoparticles could be used efficiently as first neutron reflectors covering the complete VCN energy range, thus bridging the energy gap between efficient reactor reflectors [37]

* Corresponding author.
E-mail address: nesvizhevsky@ill.eu (V.V. Nesvizhevsky).

0168-9002/$ - see front matter © 2009 Elsevier B.V. All rights reserved.
doi:10.1016/j.nima.2009.07.086

for thermal and cold neutrons, and the optical potential for UCN [38]. The first experiments on the reflection of VCN from materials containing sub-micrometer structures as well as on VCN storage were carried out in the 1970s in [39] and later continued in [40]. The use of nanoparticles provides a sufficiently large cross-section for coherent scattering with the non-homogeneity of the reflector density on a spatial scale of about the neutron wavelength. The large number of diffusive collisions needed to reflect VCN from powder constrains the choice of materials: only low-absorbing ones with high optical potential are appropriate. Thus, diamond nanoparticles were an evident candidate for such a VCN reflector. In order to measure precisely the VCN reflection probability from powder of diamond nanoparticles and to explore the feasibility of VCN storage in traps with nanostructured walls we carried out a dedicated experiment [43]. The setup is shown in Fig. 1.

The experiment was carried out at the VCN beam of PF2 at the ILL. The VCN trap has cylindrical shape with a diameter of 44 cm and a height of 47 cm. VCN could enter the trap through a small square hole of 2 cm × 2 cm in its side wall. The VCN beam diameter is ~1 cm. VCN could be reflected many times from the trap walls. Thus they could find an exit circular hole with a diameter of 6 cm in the trap cover and enter a detector behind the window. The VCN beam could be opened or closed using a fast cadmium valve with a thickness of 0.2 mm. The VCN velocity could be chosen using a velocity selector in front of the valve. The trap is placed inside a vacuum chamber with an entrance quartz window with a thickness of 3 mm and an exit aluminum window with a thickness of 1 mm. When the VCN beam is closed the detector count rate decreases exponentially following the VCN density in the trap. The characteristic time of this decrease is equal to the convolution of the VCN storage and empting times. Thus we could measure the VCN storage times as a function of VCN velocity.

The trap is built using powder of diamond nanoparticles filled into aluminum tubes and assembled into a cylinder in order to get the side trap wall as shown in Fig. 1. The aluminum thickness is 20 μm. The powder (average particle size 5 nm) in the tubes is compressed; its density is equal to 0.4 g/cm^3. The trap cover consists of an aluminum disk, an aluminum circle with a height of 3 cm fixed to its perimeter, a foil with a thickness of 30 μm, and a 3 cm thick powder layer over the aluminum foil. The powder density in the trap cover is 0.3 g/cm^3. The trap bottom is covered with powder with a thickness of 3 cm compressed to a density of 0.3 g/cm^3.

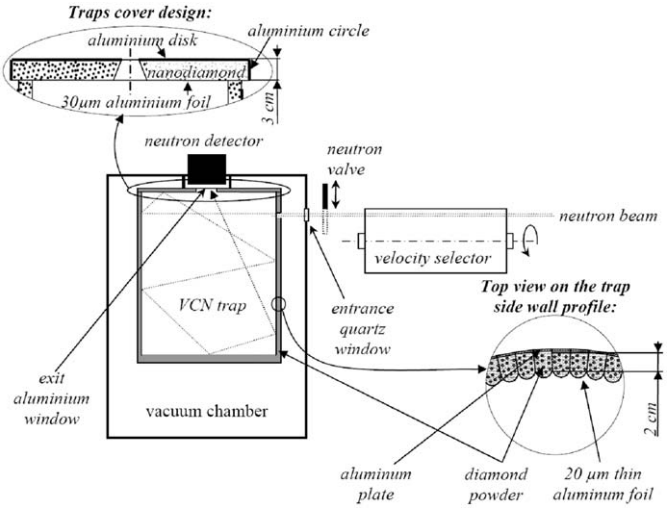

Fig. 1. The scheme of the installation used to store VCN.

The probability of VCN reflection from the trap wall could be estimated from

$$\rho(\upsilon) = 1 - \frac{\Delta x}{\tau_{st}^{VCN}(\upsilon)\upsilon}(1 - \varepsilon(\upsilon)), \quad (1)$$

where Δx is the mean free path of neutron in the trap, $\tau_{st}^{VCN}(\upsilon)$ is the storage time for neutrons with velocity υ, and $\varepsilon(\upsilon)$ is a small correction accounting for VCN losses in the entrance and exit windows as well as in aluminum foils. Measured and calculated reflectivities are shown in Fig. 2 in comparison with that for other existing neutron reflectors. As is clear from Fig. 2, the maximum energy of reflected VCN and the reflection probability by far exceed the corresponding values for the best supermirrors available [41].

The difference between theory and experimental data in Fig. 2 might be due to VCN inelastic scattering on hydrogen atoms in the powder of diamond nanoparticles. Further improvement of the VCN storage times could then be achieved by removing a part of the hydrogen from the powder in order to suppress the inelastic up-scattering of VCN. Another option consists in replacing the diamond nanoparticles by O_2, D_2, D_2O, CO_2, CO or other low-absorbing nanoparticles, free of hydrogen and other impurities with significant VCN loss cross-section.

This phenomenon has a number of applications, including storage of VCN in closed traps, reflectors for VCN and UCN sources, more efficient guiding of VCN and, probably, of even faster neutrons at "quasi-specular" trajectories.

3. Quasi-elastic scattering of UCN by nanoparticles on surfaces

In contrast to the previous case, nanoparticles bound weakly on a surface reflect neutrons quasi-elastically.

In order to measure the probability of quasi-elastic scattering of UCN, we used the gravitational spectrometer shown in Fig. 3. A sample (1) is installed on the bottom of its open storage trap. The trap side walls (2) with a height of 50 cm provide a gravitational barrier for UCN. UCN enter the trap from a neutron guide and

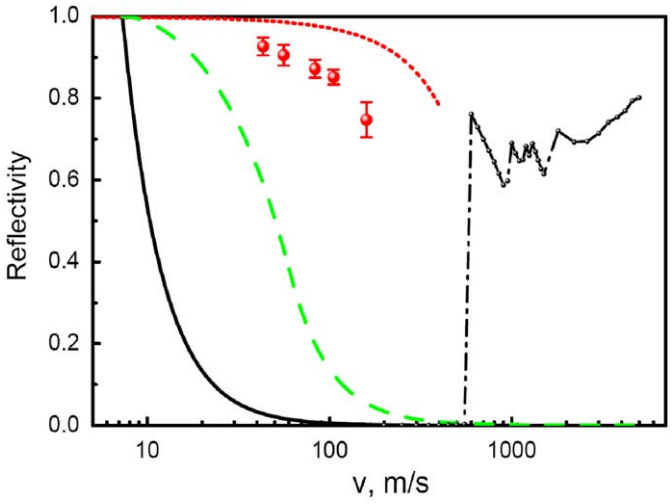

Fig. 2. The elastic reflection probability for an isotropic neutron flux is shown as a function of neutron velocity for various carbonbased reflectors: (1) diamond-like coating (DLC) (thin solid line). (2) The best supermirror [41] (dashed line). (3) Hydrogen-free ultradiamond [42] powder with infinite thickness (calculated dotted line). (4) VCN reflection from ~3 cm thick diamond nanopowder at ambient temperature (circles) with significant hydrogen contamination (experiment, this paper). (5) MCNP calculation for reactor graphite reflector [37] at ambient temperature with infinite thickness (dash-dotted line). It is assumed that the neutron energy does not increase at reflection.

could be enclosed there using a valve (3). Stored UCN pass through a small calibrated hole (4) in the trap bottom to a detector (5); thus the UCN density in the trap is measured. An absorber (6) removes all UCN with energy large enough to leave the trap above the gravitational barrier (2); then the absorber is lifted to a large height. Some stored UCN could gain energy due to quasi-elastic reflections. Such neutrons could leave the trap above the gravitational barrier and thus they could be measured in a detector (7). Knowing the number of UCN collisions with the sample surface, the number of UCN measured in the detector (7), and the efficiency of their detection, we can calculate the probability of UCN quasi-elastic scattering from the energy range 0–50 neV to the energy range 50–170 neV, as well as the spectrum of scattered neutrons.

Fig. 4 shows results of a measurement of such small heating of UCN on a stainless steel surface at various sample out-gassing temperatures [22]. Here, the average UCN energy is 30 neV, VUCN (Vaporizing UCN) energy is ~80 neV, and the energy transfer is ~50 neV. A similar increase of the probability of small heating was observed on Cu as well.

Here we present a study of nanoparticle formation on solid surfaces as a function of surface heating using an atomic-force microscope (AFM). As is clear from Fig. 4, the heating of stainless steel samples just to the temperature of the observed increase in the small heating probability is accompanied by formation of a small granular structure with a characteristic grain radius of ~5–10 nm. In total more than 400 measurements were carried out with samples of stainless steel, Cu, Fe, and Pb as well as with sapphire and silica plates at various temperatures and various sample preparation conditions. In all cases analogous surface behavior was observed. A characteristic example of a measurement of stainless steel surface is shown in Fig. 5. It demonstrates formation of nanostructures/nanoparticles on the surface in the vicinity of the outgasing temperature corresponding to the increase in the small heating probability in Fig. 4. If the small heating is due to quasi-elastic scattering of UCN on surface iron or iron-oxide nanoparticles in a state of thermal motion at ambient temperature, then their velocity should be equal to ~0.6 m/s; thus their size is 5–10 nm. Larger outgasing temperature corresponds to larger characteristic size of observed nanoparticles. An analogous effect (at different temperatures) is observed for all other studied materials.

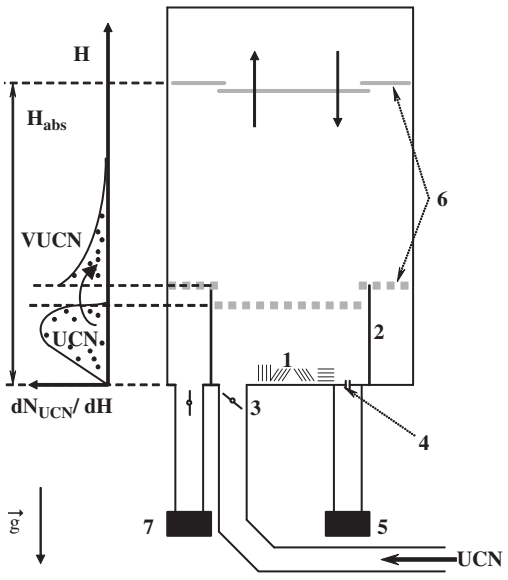

Fig. 3. Experimental set up: 1—sample, 2—gravitational barrier, 3—entrance valve, 4—monitor, 5—absorber, 6—detector, 7—exit valve, 8—calibration hole.

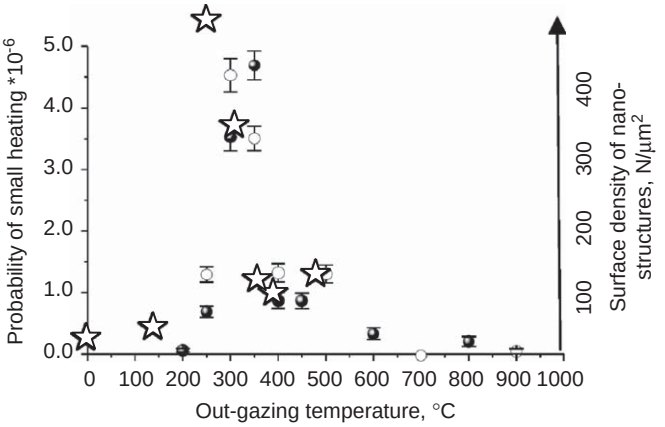

Fig. 4. The probability of small heating of UCN at stainless steel samples (alloy AISI 304) is shown as a function of the temperature of sample outgassing. The measurement is carried out at ambient temperature. The black and white points show results of two independent measurements with analogous samples. The initial UCN spectrum is shaped to the range of 0–50 neV. The probability of small heating is defined as the number of neutrons scattered to energy higher than 55 neV per wall collision.
The surface density of nanostructures (at analogous stainless steel samples) with a lateral size of 5–10 nm and a height of ~5 nm is shown with stars; the error bars are equal to their size.

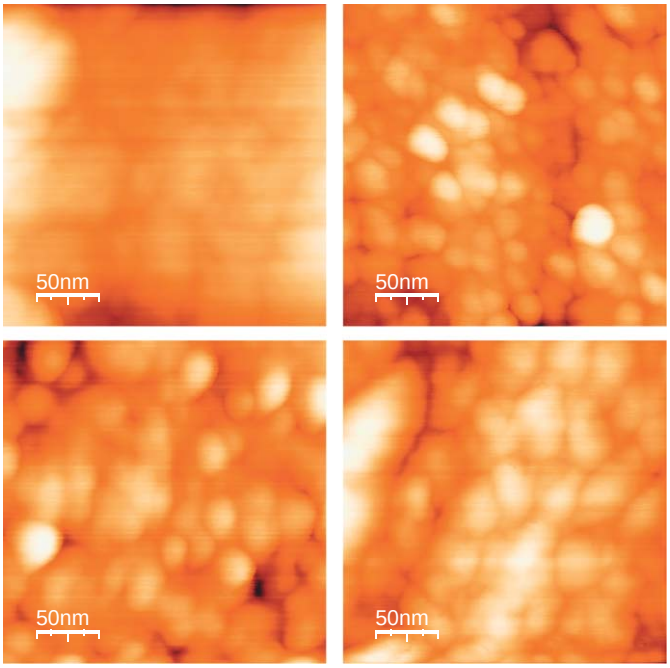

Fig. 5. Typical AFM images of surface of AISI 304 alloy foil measured as a function of a temperature of the sample heating: 20, 280, 330, 500 °C. The measurement is performed at ambient temperature.

This mechanism of small heating of UCN on solid surfaces might have a more general nature. A large Fomblin molecule is a nanoparticle with the characteristic size of a few nanometers, providing a scattering potential density contrast visible in standard neutron scattering experiments. It is affected by thermal motion, thus leading to quasi-elastic UCN reflection. Due to its high mobility it could produce significant effects.

In precision neutron lifetime experiments, small heating of UCN on liquid and solid surfaces may produce large systematic effects if not properly monitored during measurements.

4. Conclusion

We have demonstrated that intense scattering of VCN in the bulk of powder of diamond nanoparticles provides an efficient albedo of VCN. This phenomenon has a number of applications, including storage of VCN in closed traps, reflectors for VCN and UCN sources, and more efficient guiding of VCN. On the other hand, scattering of nanoparticles bound weakly on surface results in small heating of UCN in storage experiments; it could result in the appearance of false effects in neutron lifetime measurements.

Acknowledgement

The work was supported in part by CRDF Grant RUP1-2841-CG-061.

References

[1] C.A. Baker, et al., Phys. Rev. Lett. 97 (2006) 131801.
[2] I.S. Altarev, Phys. Lett. B 276 (1992) 242.
[3] J. Baumann, et al., Nucl. Instr. and Meth. A 284 (1989) 130.
[4] Yu.V. Borisov, et al., J. Tech. Phys. 58 (1989) 951.
[5] H. Abele, et al., Phys. Rev. Lett. 88 (2002) 211801.
[6] M. Schumann, et al., Phys. Rev. Lett. 99 (2007) 191803.
[7] S. Arzumanov, et al., Phys. Lett. B 483 (2000) 15.
[8] V.V. Nesvizhevsky, et al., Nature 415 (2002) 297.
[9] V.V. Nesvizhevsky, et al., Phys. Rev. D 67 (2003) 102002.
[10] V.A. Vesna, et al., Phys. Rev. C 77 (2008) 035501.
[11] T. Soldner, et al., Phys. Lett. B 581 (2004) 49.
[12] V.V. Nesvizhevsky, et al., Eur. J. Appl. Phys. 6 (1999) 151.
[13] V.V. Nesvizhevsky, et al., Phys. At. Nucl. 62 (1999) 776.
[14] A.V. Strelkov, et al., Nucl. Instr. and Meth. A 440 (2000) 695.
[15] E.V. Lychagin, et al., Phys. At. Nucl. 63 (2000) 548.
[16] V.V. Nesvizhevsky, et al., Phys. Lett. B 479 (2000) 353.
[17] V.V. Nesvizhevsky, Phys. At. Nucl. 65 (2002) 400.
[18] E.V. Lychagin, et al., Phys. At. Nucl. 65 (2002) 1995.
[19] V.V. Nesvizhevsky, Phys. Usp. 46 (2003) 93.
[20] L.P. Mezhov-Deglin, V.V. Nesvizhevsky, A.V. Stepanov, Phys. Usp. 46 (2003) 89.
[21] V.V. Nesvizhevsky, G. Pignol, K.V. Protasov, IJN 6 (2007) 485.
[22] D.G. Kartashov, et al., IJN 6 (2007) 501.
[23] L.P. Mezhov-Deglin, et al., JLTP 148 (2007) 833.
[24] L.P. Mezhov-Deglin, et al., JLTP 150 (2008) 206.
[25] E.V. Lychagin, et al., Surf.: Rent., Synch. Neut. Invest. 7 (2002) 81.
[26] V.I. Luschikov, et al., JETP Lett. 9 (1969) 23.
[27] P. Ageron, et al., Z. Phys. B 59 (1985) 261.
[28] V.P. Alfimenkov, et al., JETP Lett. 55 (1992) 84.
[29] V.K. Ignatovich, The Physics of Ultracold Neutrons, Clarendon Press, Oxford, 1991.
[30] R. Golub, D.J. Richardson, S.K. Lamoreaux, Ultracold Neutrons, Adam Higler, Bristol, 1991.
[31] A.V. Strelkov, Lectures of IV International School on Neutron Physics, Alushta, JINR, Dubna, 1991 p. 325.
[32] L.N. Bondarenko, et al., JETP Lett. 68 (1998) 691.
[33] S.S. Arzumanov, et al., in: Proc. ISINN-10, 2002, 356.
[34] L.N. Bondarenko, et al., Phys. At. Nucl. 65 (2002) 11.
[35] A.P. Serebrov, et al., Phys. Lett. A 309 (2003) 218.
[36] A. Steyerl, et al., Eur. Phys. J. B 28 (2002) 299.
[37] E. Fermi, A course in neutron physics?, in: Collected Papers, The University of Chicago Press, Chicago, 1965.
[38] V.V. Nesvizhevsky, et al., arXiv:0805.2634/nucl-ex, 2008.
[39] A. Steyerl, W.-D. Trustedt, Z. Phys. 267 (1974) 379.
[40] S.S. Arzumanov, et al., Phys. At. Nucl. 68 (2005) 1141.
[41] R. Maruyama, et al., Thin Solid Films 515 (2007) 5704.
[42] 〈http://www.ultradiamondtech.com〉.
[43] E.V. Lychagin, et al., Phys. Lett. B 679 (2009) 186.
[44] V.A. Artemiev, Перспективные материалы 6 (2008) 121.
[45] V.V. Nesvizhevsky, G. Pignol, K.V. Protasov, Phys. Rev. D 77 (2008) 034020.